



Actinide chemistry in aqueous solutions for waste disposal and environmental studies.

by Pierre Vitorge^{1,2}

Catherine Beaucaire², Colin Marsden³, Michael Descostes², Dominique You², Patrick Lovera², H el ene Capdevila⁴

(1) UMR 8587 Universit e d'Evry-CNRS-CEA².pierre.vitorge(at)cea.fr.

(2) CEA DEN Saclay DPC/SECR, F91191 Gif sur Yvette cedex, France

(3) LPQ IRSAMC Universit e Paul Sabatier, 118 route de Narbonne, F31062 Toulouse cedex4, France

(4) CEA DEN Cadarache DTCD/SPDE ,13108 Saint-Paul-lez-Durance cedex, France

1. Introduction

The solubilities of radionuclides in groundwaters can be increased by the formation of soluble complexes, which also lowers their retention on surfaces of natural minerals and engineered barriers. This has been studied for managing radioactive wastes, typically for possible deep disposals, an option for long live radionuclides such as minor Actinides. Beside basic knowledge on redox, hydrolysis and complexing chemical equilibria of Actinides and analogue hard cations, these studies provided few methodological developments useful for many other elements, and for the chemical scientific community. In this paper, we outline some of these methodologies through examples for solution chemistry of Actinide chemistry.

Equilibrium Aqueous Speciation, the ratios of the soluble species is currently predicted by Thermodynamics, namely Mass Action Law as reflected by equilibrium constants K , at given temperature T , and pressure P . This is well established for ideal systems –typically at constant high ionic strength I - providing numerical values of K 's are known. In a first part we show examples in nature and in laboratory, where mass action law was used for interpreting experimental data, or for producing Gibbs energies of reactions Δ_rG ($=-RT\ln K$). We then indicate further Thermodynamics developments:

- activity coefficients for extrapolating to zero ionic strength, the standard state,
- solid solutions for predicting retention of trace elements; dissolution of solid solutions can be interpreted as reactions of two advancement variables, one of them typically for the corresponding ionic exchange equilibrium; conversely any ionic exchange equilibrium can be implicitly associated with the dissolution/precipitation reactions of the matrix supporting the ionic exchange sites,
- comparing semi-empirical formula used for activity coefficients and surface complexation, since they both derive from similar physical models.

When K values are not known, chemical analogies can be used for estimating them, as typically for the stabilities of PuO_{2+x} compounds. Finally we discuss the using of molecular modelling and ab initio calculations for understanding solution coordination chemistry.

2. THERMODYNAMICS

2.1 Speciation

In this Section we illustrate Mass Action Law is experimentally validated in natural systems and in laboratory experiments. **Aqueous speciation in deep groundwaters** is usually controlled by the geological media, *i.e.* by solid compounds usually formed by precipitation after and during the lixiviation of original minerals. This is used by geochemists for understanding and even modelling aqueous speciation: Figure 1 typically illustrates such control for Stripa groundwaters [96TRO, 00BEA, 02COU and 03BEA].

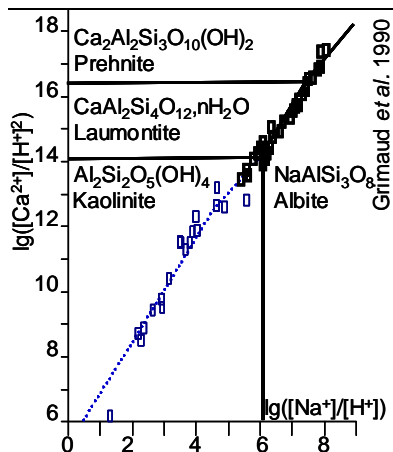


Figure 1 Equilibration of groundwaters.
 From chemical analysis on Stripa groundwaters their equilibration with minerals and their slow evolution were modelled by using Mass Action Law [90GRI]. In the upper part of the phase diagram (bolded black points and solid straight lines), the experimental dots appeared to be on the frontiers between the stability domains of Albite and Laumontite or Prehnite, while in the kaolinite domain the dotted line was calculated from an evolution model based on Charge Balance Equation. Values of solubility products K_s 's, have been re-fitted on the experimental observations; however, these changes in K_s values are within usual uncertainties for solid compounds formed at low temperatures: less than $0.6 \log_{10}$ unit (i.e. $0.3 \text{ kJ}\cdot\text{mol}^{-1}$ on $\Delta_r G$) as compared to Ref. [83MIC].

Similar approaches are used in laboratory for modelling Radionuclide Speciation and deducing equilibrium constants (Figure 2); providing equilibrium conditions are achieved, and the chemical system is ideal (within experimental accuracy): Mass Action Law quantitatively models Aqueous Speciation and Solubility in deep groundwaters (Figure 1) and in laboratory experiments (Figure 2). For making aqueous solutions ideal high and constant concentration of an inert electrolyte is classically used: high Na^+ concentration was typically used for the data reported in Figure 2, which allowed sensitivity analysis, i.e. testing all possible stoichiometries for soluble complexes $(\text{NpO}_2)_p(\text{CO}_3)_q(\text{OH})_r^{p-2q-r}$. This type of approach is classical; however, it has always been debated, whether adding new minor species is meaningful, i.e. are the fitted values of their formation constants meaningful, or do they only "fit the uncertainty". Alternatively, we proposed to only estimate maximal possible values for such formation constants (see typically Ref. [01LEM and 03VIT]), this also allows finding chemical conditions, in which such minor species should eventually be better evidenced.

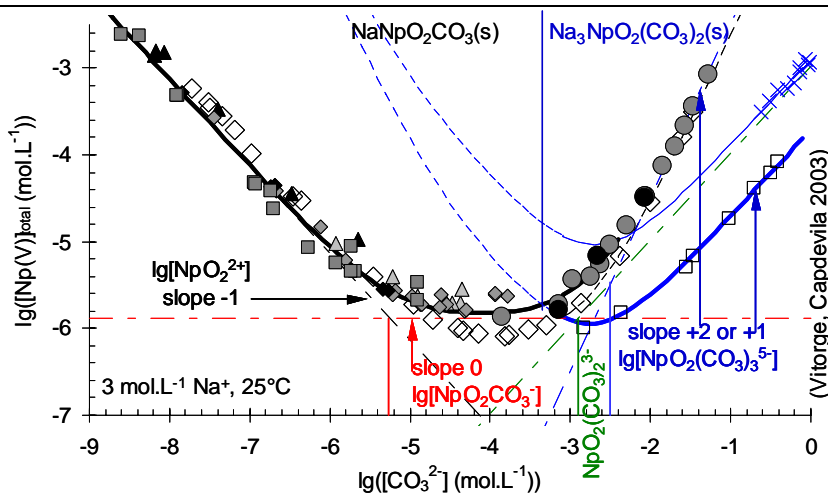


Figure 2: Np(V) solubility in $\text{CO}_3^{2-} / \text{HCO}_3^- / \text{CO}_2$ aqueous solutions.

Np(V) solubilities were measured in our laboratory in various pH conditions -grey and black points- [84VIT, 85COM, 85KIM, 86GRE, 89RIG, 98VIT and 03VIT] and in other laboratories. All the published experimental data on this system were reviewed and eventually quantitatively reinterpreted with a single chemical model [98VIT] in the course of the NEA TDB project [01LEM]. When $\lg[\text{CO}_3^{2-}] < -5$, experimental solubilities are on a straight line of slope -1: this, and the other slope analysis written on the figure illustrates Mass Action Law accounts for the experimental solubilities, even in oversaturated solutions (dashed lines) i.e. before the transformation of $\text{NaNpO}_2\text{CO}_3(\text{s})$ into $\text{Na}_3\text{NpO}_2(\text{CO}_3)_2(\text{s})$.



2.2 Activity coefficients

Activity coefficients γ 's, are classically introduced for comparing the values of an equilibrium constant measured in different aqueous ionic media, and for extrapolating to zero ionic strength; however there is no international conventions on the way to obtain the numerical values of the activity coefficients, despite they actually define Standard State -zero ionic strength or equivalently infinite dilution- for aqueous solutions. We tested several formula for calculating γ 's [87RIG, 87ROB and 89RIG], typically Debye-Hückel and Davies formula can only be used for $I < 0.01$ and 0.1 mol.L^{-1} respectively in aqueous solutions, while in more concentrated ionic media empirical fitted parameters are needed. We used **SIT Formula** for calculating γ_i , the activity coefficient of ion i , with charge z_i

$$\lg \gamma_i = -z_i^2 D + \varepsilon_{ij} m_j \quad 1$$

where $D = A I_m^{0.5} / (1+B I_m^{0.5})$ is Debye-Hückel Term, $A = 0.509 \text{ kg}^{0.5} \cdot \text{mol}^{-0.5}$ and $B = 1.5 \text{ kg}^{0.5} \cdot \text{mol}^{-0.5}$ at 25°C [O1LEM], I_m is molal ($\text{mol} \cdot \text{kg}^{-1}$) I , m_j is the molal concentration ($\text{mol} \cdot \text{kg}^{-1}$) of ion j , ε_{ij} is an empirical fitted parameter for ions i and j , $z_i z_j < 0$, j is the major ion (if needed summation on j is performed), this usual notation is confusing, since ε_{ij} is not a dielectric constant. Reporting SIT Formula into the definition of equilibrium constant K ,

$$\lg K^\circ = \lg K_m - \Delta z^2 D + \Delta \varepsilon m \quad 2$$

where K° is the K value at zero ionic strength, m is the molality of the salt used to maintain constant high ionic strength, K_m is K value using molal units, $\Delta z^2 = \sum_i \nu_i z_i^2$, $\Delta \varepsilon = \sum_i \nu_i \varepsilon_{ij}$, ν_i 's are the stoichiometric coefficients for the reaction of Equilibrium constant K , and Term $\nu_{\text{H}_2\text{O}} a_{\text{H}_2\text{O}}$ is eventually included in Term $\Delta \varepsilon m$. These formulas

- can be used at up to $4 \text{ mol} \cdot \text{kg}^{-1}$ concentrations even for aqueous ions highly charged –typically Pu^{4+} (Figure 3 and Figure 4) or $\text{NpO}_2(\text{CO}_3)_3^{5-}$,
- only one parameter -namely ε_{ij} - is used for each ion pair, it is symmetric ($\varepsilon_{ij} = \varepsilon_{ji}$) which allows simplifications as typically using the same ion pair fitted parameters for trace and macro concentrations, conversely this simplification is not consistent when higher order terms –typically proportional to m_j^2 - are added,
- it was adopted by the NEA TDB reviews.

We tested the SIT formula on several systems: Actinides in non complexing [87RIG, 89RIG2, 90CAP, 92CAP, 95CAP and 98CAP] and carbonate media [86GRE, 90CAP, 92CAP, 96CAP, 98RIG and 99CAP]. Extrapolating to zero ionic strength by using the SIT formula was illustrated for $E_{\text{Pu}^{4+}/\text{Pu}^{3+}}$, the potential of the $\text{Pu}^{4+}/\text{Pu}^{3+}$ redox couple measured at 25°C (Figure 3): despite Pu^{4+} and Pu^{3+} are quite highly charged species $\Delta \varepsilon_{\text{Pu}^{4+}/\text{Pu}^{3+}}$ appears to be constant to surprisingly high ionic strength. This is actually only plotted for $\Delta \varepsilon_{\text{Pu}^{4+}/\text{Pu}^{3+}} = \varepsilon_{\text{Pu}^{3+}} - \varepsilon_{\text{Pu}^{4+}}$ on Figure 3; however, this was as well observed for $\varepsilon_{\text{Pu}^{4+}}$ and $\varepsilon_{\text{Pu}^{3+}}$ each alone (Figure 4). For applications, beside **ionic strength corrections**, **temperature corrections** are needed. Among others, SIT Formula can be used at any constant temperature T , for extrapolating K –including normal potentials $E_{\text{ox/red}}$ (Figure 3)- giving $K^\circ(T)$ and $\Delta \varepsilon(T)$ at $T = 298.15 \text{ K}$ (*i.e.* 25°C). At other temperatures quite few K values are published, and even fewer $\Delta \varepsilon(T)$ values: we measured some of them in narrow temperature ranges (Figure 5).

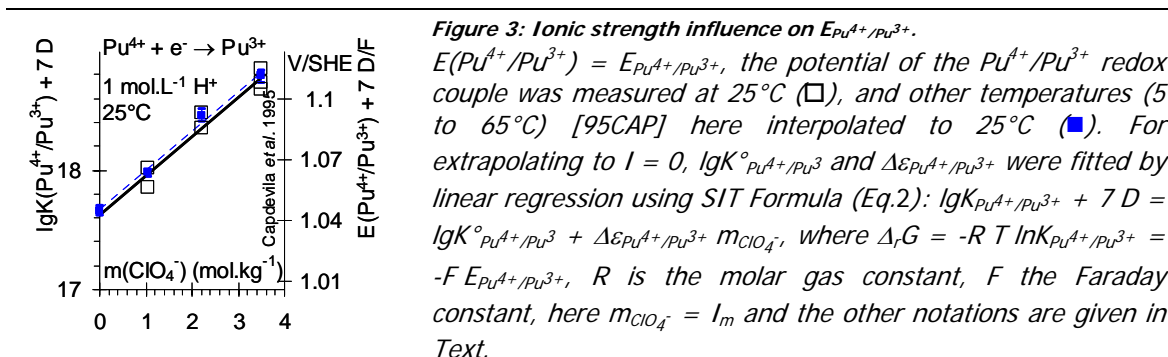


Figure 3: Ionic strength influence on $E_{Pu^{4+}/Pu^{3+}}$.

$E(Pu^{4+}/Pu^{3+}) = E_{Pu^{4+}/Pu^{3+}}$, the potential of the Pu^{4+}/Pu^{3+} redox couple was measured at 25°C (\square), and other temperatures (5 to 65°C) [95CAP] here interpolated to 25°C (\blacksquare). For extrapolating to $I = 0$, $lgK^{\circ}_{Pu^{4+}/Pu^{3+}}$ and $\Delta\varepsilon_{Pu^{4+}/Pu^{3+}}$ were fitted by linear regression using SIT Formula (Eq.2): $lgK_{Pu^{4+}/Pu^{3+}} + 7D = lgK^{\circ}_{Pu^{4+}/Pu^{3+}} + \Delta\varepsilon_{Pu^{4+}/Pu^{3+}} m_{ClO_4^-}$, where $\Delta_rG = -RT \ln K_{Pu^{4+}/Pu^{3+}} = -F E_{Pu^{4+}/Pu^{3+}}$, R is the molar gas constant, F the Faraday constant, here $m_{ClO_4^-} = I_m$ and the other notations are given in Text.

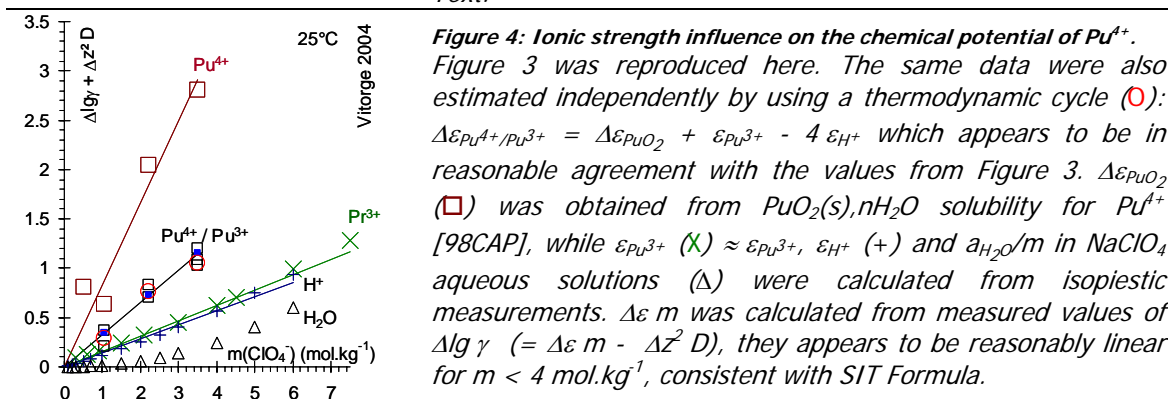


Figure 4: Ionic strength influence on the chemical potential of Pu^{4+} .

Figure 3 was reproduced here. The same data were also estimated independently by using a thermodynamic cycle (\circ): $\Delta\varepsilon_{Pu^{4+}/Pu^{3+}} = \Delta\varepsilon_{PuO_2} + \varepsilon_{Pu^{3+}} - 4\varepsilon_{H^+}$ which appears to be in reasonable agreement with the values from Figure 3. $\Delta\varepsilon_{PuO_2}$ (\square) was obtained from $PuO_2(s), nH_2O$ solubility for Pu^{4+} [98CAP], while $\varepsilon_{Pu^{3+}}$ (\times) $\approx \varepsilon_{Pu^{3+}}$, ε_{H^+} ($+$) and a_{H_2O}/m in $NaClO_4$ aqueous solutions (Δ) were calculated from isopiestic measurements. $\Delta\varepsilon m$ was calculated from measured values of $\Delta lg \gamma$ ($= \Delta\varepsilon m - \Delta z^2 D$), they appears to be reasonably linear for $m < 4 \text{ mol.kg}^{-1}$, consistent with SIT Formula.

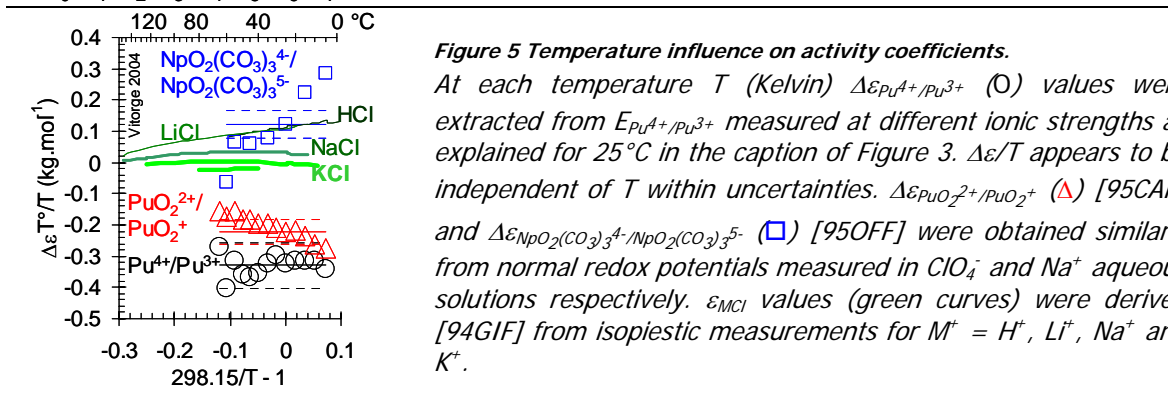


Figure 5 Temperature influence on activity coefficients.

At each temperature T (Kelvin) $\Delta\varepsilon_{Pu^{4+}/Pu^{3+}}$ (\circ) values were extracted from $E_{Pu^{4+}/Pu^{3+}}$ measured at different ionic strengths as explained for 25°C in the caption of Figure 3. $\Delta\varepsilon/T$ appears to be independent of T within uncertainties. $\Delta\varepsilon_{PuO_2^{2+}/PuO_2^+}$ (Δ) [95CAP] and $\Delta\varepsilon_{NpO_2(CO_3)_3^{4-}/NpO_2(CO_3)_3^{5-}}$ (\square) [95OFF] were obtained similarly from normal redox potentials measured in ClO_4^- and Na^+ aqueous solutions respectively. ε_{MCl} values (green curves) were derived [94GIF] from isopiestic measurements for $M^+ = H^+, Li^+, Na^+$ and K^+ .

We also proposed SIT based equations for modelling temperature influence on γ 's, or equivalently for **ionic strength corrections on Δ_rH , Δ_rS and Δ_rC_p** [93GIF]. In the SIT formula $\Delta\varepsilon m$ term is introduced as a virial expansion, or equivalently from van der Waals Equation for gas: in both cases this term is predicted to be proportional to m/T –not only m -; to our knowledge, this was not really systematically tested in literature. However, we plotted experimental values of $\Delta\varepsilon/T$, or equivalently $\Delta\varepsilon T^{\circ}/T$ (Figure 5). There are no data on enough experimental systems to draw general conclusions. However $\Delta\varepsilon_{Pu^{4+}/Pu^{3+}} T^{\circ}/T$ values are constant within uncertainty, and no trend with T can be inferred. This is less clear for $\Delta\varepsilon_{PuO_2^{2+}/PuO_2^+} T^{\circ}/T$, which slightly increases with T , a tendency not confirmed for MCl strong electrolytes, for which data are available at higher temperatures (at equilibrium H_2O partial pressure), while $m \Delta\varepsilon_{NpO_2(CO_3)_3^{4-}/NpO_2(CO_3)_3^{5-}}$ appears to vary with T , which might reflect ion pairing at low T , as we already suggested for $UO_2(CO_3)_3^{5-}$, a species analogous to $NpO_2(CO_3)_3^{5-}$ [89RIG]. Nevertheless, assuming $\varepsilon_T = \varepsilon_T^{\circ} T^{\circ}/T$ seems a **reasonable approximation** for extrapolating activity coefficients in the range 0 to 150°C from data at 25°C without any new fitted parameter, and this did not increase uncertainties dramatically for most of the above systems:

horizontal straight lines in Figure 5 are mean values $\pm 1.96\sigma$ (dashed lines) measured at 25°C. This was not specially expected since fitted parameters $-i.e.$ ϵ 's and $\Delta\epsilon$'s- have not necessarily the physical meaning used to introduce them in semi-empirical formulas: ϵ numerical values might very well fit approximations used for obtaining SIT Formula. At **higher temperatures** our estimations of $\Delta\epsilon$ values are certainly not much accurate. They were obtained by subtracting $\Delta z^2 D$ (a Debye-Hückel term) from measured $\Delta \lg \gamma$'s (see Eq.2 and the caption of Figure 3), where for calculating D values at different temperatures, A and B parameters were taken from Ref.[01LEM]. However it is not clear whether ρ , the molar to molal conversion factor is actually taken into account in literature, while it should be since $A = be^2/(8\pi dkT)$, $b = e(2000N_A/(\rho dkT))^{0.5}$, where $B = b r$, d is the dielectric constant (we are avoiding the more usual notation ϵ , since it is already used for SIT ion pair coefficients), k is Boltzman Constant, e is the elementary charge, N_A is Avogadro Number and r is the ionic radius assumed to be the same for any ion, and here assumed to be independent from T.

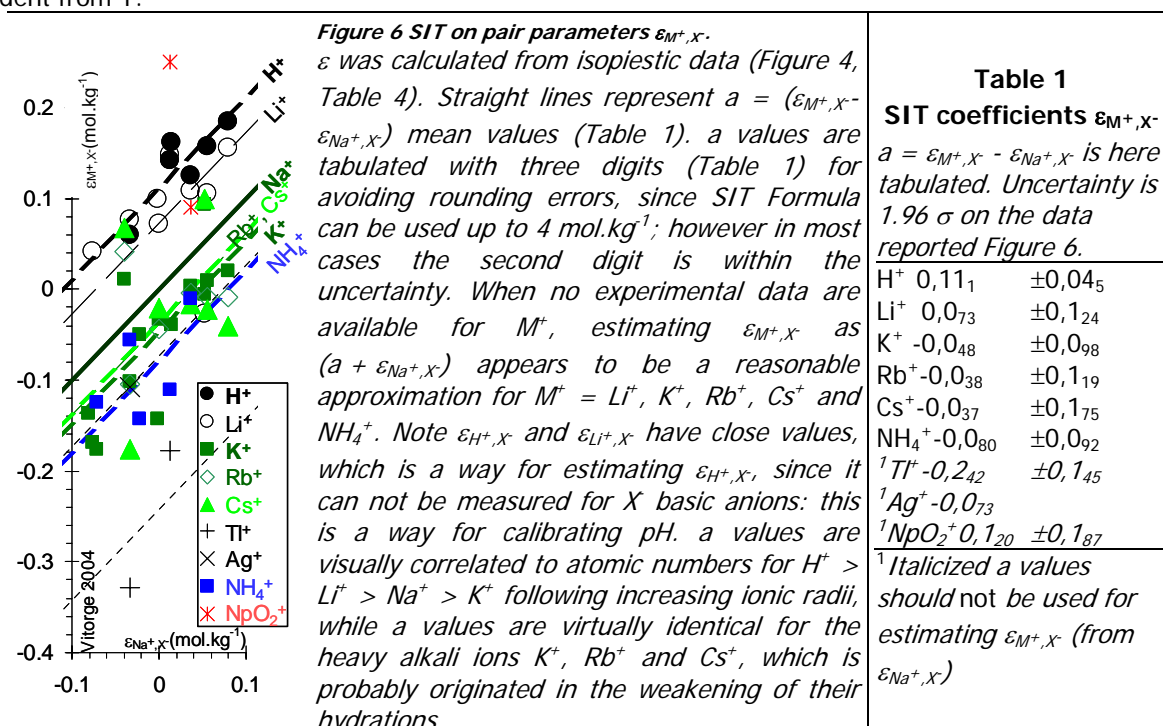


Table 1
SIT coefficients ϵ_{M^+,X^-}
 $a = \epsilon_{M^+,X^-} - \epsilon_{Na^+,X^-}$ is here tabulated. Uncertainty is 1.96 σ on the data reported Figure 6.

H ⁺	0,11 ₁	$\pm 0,04_5$
Li ⁺	0,07 ₃	$\pm 0,12_4$
K ⁺	-0,04 ₈	$\pm 0,09_8$
Rb ⁺	-0,03 ₈	$\pm 0,11_9$
Cs ⁺	-0,03 ₇	$\pm 0,17_5$
NH ₄ ⁺	-0,08 ₀	$\pm 0,09_2$
¹ Tl ⁺	-0,24 ₂	$\pm 0,14_5$
¹ Ag ⁺	-0,07 ₃	
¹ NpO ₂ ²⁺	0,12 ₀	$\pm 0,18_7$

¹ Italicized a values should not be used for estimating ϵ_{M^+,X^-} (from ϵ_{Na^+,X^-})

Finally, ϵ coefficients, the ion pair parameters seem to reproduce reasonably well temperature influence on experimental $\Delta \lg \gamma$ values, despite they were fitted at constant temperature (25°C) for reproducing ionic strength $- \log I$ influence: this was not specially expected, since fitted ϵ coefficients certainly fit several physical phenomena not taken into account in the physical demonstration of SIT Formula, these phenomena were known to vary as ϵI , they appear to also vary as $\epsilon I / T$. It is certainly not understood, why SIT Formula is valid in these I and T domains. Nevertheless, it can easily be used for applications providing ϵ values are available: we tabulated several of them (Table 3 and Table 4) see also Ref.[01LEM]. ϵ values can be estimated by analogy with similar ions of similar effective charge z , and size (Figure 6, Figure 7 and Figure 8) for $-4 < z < +4$.

2.3 Formation data for e-

Identifying consistent Reference State is needed, when using data from different scientific communities; typically e^- , the notation of electrochemists actually corresponds to $E = -(RT/F) \ln a_{e^-}$, where E is the redox potential of the solution, and a_{e^-} the activity of e^- : when E is measured vs. SHE, for consistency with the usual reference state

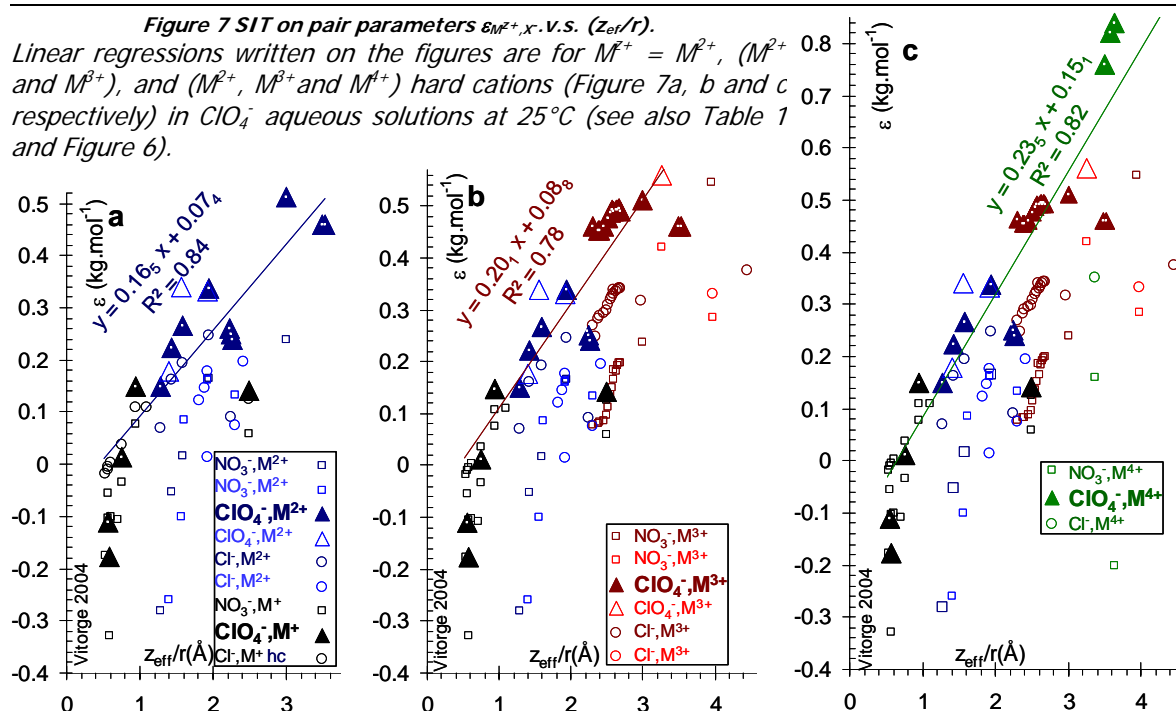
$$\Delta_f X_{e^-} = 0.5 \Delta_f X_{H_2(g)} - \Delta_f X_{H^+(aq)}$$



where X is a thermodynamic function, typically G, H [94GIF], and subscript f, means formation. $\Delta_f G_i$ is another notation for μ_i° , the standard chemical potential of species i. ϵ Notation is useful for ionic strength corrections [01LEM], and for charge balance, nevertheless this notation is not always accepted, moreover $\Delta_f G_{H^+(aq)} = 0$, a usual convention might be quite misleading. For clarity, we now recall usual conventions.

Thermochemical data bases often tabulate $\Delta_f G$, $\Delta_f H$, S, C_p at 25°C and eventually coefficient for computing T dependency of C_p by using these coefficients in empirical formula. As for any element in the reference state, $\Delta_f G_{H_2(g)} = 0$ and $\Delta_f H_{H_2(g)} = 0$, i.e. $H_2(g)$ is the reference state for Element H. $\Delta_r X_i$ is $\Delta_r X_i$ (subscript r, means reaction) for the reaction, where a product is Species i, and all the other reactants and products are species in their reference state. Since $\Delta_r S = (\Delta_r H - \Delta_r G)/T$, $\Delta_r S_{H_2(g)} = 0$; however, $\Delta_r S$ is not usually tabulated, while one usually tabulates S, the entropy values at 25°C consistent with the third principle of thermodynamics (Entropy is 0 at 0 K). Typically $S_{H_2(g)}$ is not zero.

Only neutral species have been chosen in the reference state, which cannot generate charged species, however SHE Convention is a way to generate ions. $\Delta_f G_{H^+(aq)} = 0$ and $\Delta_f H_{H^+(aq)} = 0$ are often written, which might be misleading: the reference state for Element H, is $H_2(g)$, not $H^+(aq)$. Notation (aq) is usually omitted, however $H^+(aq)$ –not H^+ - data are usually tabulated in thermochemical databases, which can be checked by calculated the standard ionic product of water at 25°C ($10^{-14.00}$) from $\Delta_f G_{OH^-(aq)}$ and $\Delta_f G_{H_2O(l)}$. However $S_{H^+} = 0$ is often tabulated, which actually means $S_{H^+(aq)} = 0$ at 25°C –not at 0 K. This is perfectly correct, but quite misleading, specially when 0 is ab initio calculated for H^+ , since H^+ has no electron.



Smaller symbols are used for non hard cations. Figure 7a is reproduced in Figure 7b where M^{3+} ions are added, similarly M^{4+} ions are added in Figure 7c. Linear regression were performed only for hard cations in ClO_4^- media, since the other systems might not correspond to strong electrolytes. r is ionic radius of M in solid compounds [88WEA], z_{ef} is the charge z , of cation M^{z+} , while $z_{ef} = z-1$ for MO_2^{z+} cations (actinides). The $\epsilon_{M^{z+}, X}$ values were calculated for 4 molal aqueous solutions when available, or taken from the NEA-TDB [01LEM]. These figures can be used for estimating unknown ϵ values and corresponding uncertainties for similar ions, even for complexes [01LEM].

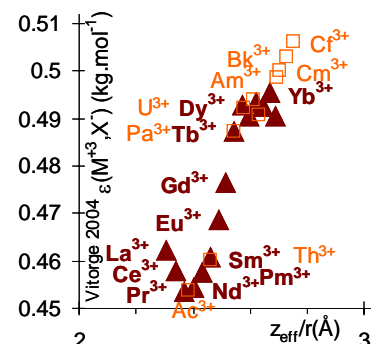


Figure 8 Estimating $\varepsilon_{An^{3+}, ClO_4^-}$
 This is a detail of Figure 7c for Lanthanide trications, where $\varepsilon_{An^{3+}, ClO_4^-}$, the corresponding values for Actinide trications have been estimating by analogy, all these numerical values are in Table 3. Non regular trend in $\varepsilon_{An^{3+}, ClO_4^-}$ v.s. Z_{eff}/r certainly reflects changes in the hydration of lanthanide trications.

Finally for consistency with usual conventions of classical thermodynamics:

- e^- , the notation of electrochemists is defined by its charge, and by a_{e^-} , its activity. Thermodynamic molal Activity is another definition of Chemical Potential; the chemical potential of e^- is actually $\mu_{e^-} = -F E = R T \ln a_{e^-}$, where E is the redox potential of the solution measured vs. SHE, and $\mu_{e^-}^\circ = \Delta_f G_{e^-} = 0$ (see below). This recalls e^- is a characteristic of the solution. In opposition to all other species, a_{e^-} is not simply related to $[e^-]$, the concentration of $e^-(aq)$, the solvated electron, despite $e^-(aq)$ can be involved in kinetic studies, as typically a consequence of the radiolysis of water. Depending on the electrodes, the domain of electroactivity of water spans over about 1 or 2 V; this corresponds to 16.90 or 33.81 \log_{10} unit of a_{e^-} respectively, since at 25°C $(RT/F)\ln 10 = 0.05916$ V.
- $\Delta_f G_{H^+} = 0$ and $\Delta_f H_{H^+} = 0$ are conventions, they actually account for the convention $0 = \Delta_f X_{ESH} = 0.5 \Delta_f X_{H_2(g)} - \Delta_f X_{H^+(aq)} - \Delta_f X_{e^-}$, where $\Delta_f X_{H_2(g)} = 0$, since $H_2(g)$ is the reference state for Element H. $\Delta_f X_{H_2(g)}$ and $\Delta_f X_{H^+(aq)}$, the two first terms in $\Delta_f X_{ESH}$ definition could in theory be calculated by dynamic ab initio calculations, since they correspond to actual species, namely $H_2(g)$ and $H^+(aq)$; however this might not be the same for $\Delta_f X_{e^-}$: for this reason a convention –as typically SHE– can be chosen. SHE Convention is not specially based on physical properties of $H^+(aq)$, neither of $e^-(aq)$ nor e^- . Actually when $\Delta_f X_{e^-}$ is omitted, it is in fact set to zero, and $\Delta_f X_{H^+(aq)} = 0$. This does not mean $H^+(aq)$ is the reference state for H. Similarly $S_{e^-} = 0.5 S_{H_2(g)} - S_{H^+(aq)}$, choosing $S_{H^+(aq)} = 0$, induces $S_{e^-} = 0.5 S_{H_2(g)}$ which is not zero at 25°C; but $S_{H_2(g)} = 0$ at 0 Kelvin.

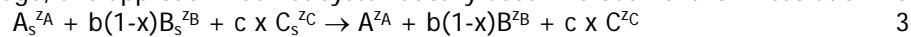
2.4 Solid Solutions

Solid solutions are solid phases of variable stoichiometries, also called non-stoichiometric compounds, typically in $AB_{b(1-x)}C_{cx}(s)$, a solid solution formed with ions A^{z_A} , B^{z_B} and C^{z_C} , where $b = -z_A/z_B$ and $c = -z_A/z_C$, the stoichiometric coefficients are $v_A = 1$, $v_B = b(1-x)$ and $v_C = cx$. When $z_B z_C > 0$, for electroneutrality $z_A z_B < 0$ and $z_A z_C < 0$; exchanging ions B^{z_B} and C^{z_C} is a way for varying the stoichiometry within the solid solution, hence at constant v_A : this is how the notations were chosen; and for this reason $b > 0$ and $c > 0$. Several approaches are used in geochemical literature for modelling solid solutions, they eventually include empirical parameters to account for experimental observations, despite more sophisticated modelling was developed for metallurgy at higher temperature.

Solid-solution dissolutions are **reactions of -at least- two advancement variables**, which, a priori, does not allow the using of the classical form for mass action law, because its classical thermodynamic demonstration involves $d[X_i] = d(v_i \xi) = v_i d\xi$ terms for minimizing $\Delta_r G$, the Gibbs energy of the reaction, where $[X_i]$ and v_i are the concentration and the constant stoichiometric coefficient for species X_i ($= A, B$ and C), and ξ is the advancement variable of the reaction. Nevertheless, equations similar to Mass Action Law are often used, and they are correct. They are usually introduced by avoiding mathematical derivations ($v_i d\xi$ terms for minimizing $\Delta_r G$); which might look like a non convincing mathematical paradox. For clarity, thermodynamic description of solid solutions can be obtained by minimizing $\Delta_r G$ in the a similar way as for the thermodynamic demonstration of Mass Action Law; which we are essentially doing in this section.



In solid solutions stoichiometric coefficients v_i , vary: new dv_i terms appear when developing $d(v_i \xi)$, which will introduce v_i' , the stoichiometric coefficients of the ionic exchange reaction corresponding to the variation of the stoichiometry of the solid solution. Conversely v_i can be obtained from v_i' : any ionic exchange equilibrium can be considered as deriving from a solid solution, which is the matrix supporting the ionic exchange sites [99VIT/BEA, 03VIT]. To our knowledge, this approach was not systematically used: we outline it for Dissolution Reaction 3



where $(A_s^{zA} + b(1-x)B_s^{zB} + c x C_s^{zC})$ is another notation for Solid Solution $AB_{b(1-x)}C_{cx}(s)$, and X_s is species X , in the solid solution. The advancement variable at constant x value is typically $\xi = [A]$: $(dX)_x = v_i d\xi$, while when x varies $dX_i = v_i d\xi + \xi dv_i$, and since $dv_i = v_i' dx$, where $v_i' = dv_i/dx$

$$dX_i = v_i d\xi + \xi v_i' dx \quad 4$$

Since $v_A' = 0$, $v_B' = -b$ and $v_C' = c$, v_i 's appear to be the stoichiometric coefficients in



a classical ionic exchange equilibrium *-i.e.* with constant stoichiometric coefficients. For stoichiometric solids (at constant value for $x = \alpha$)

$$\Delta_r G_{s\alpha}^\circ = -RT \ln K_{s\alpha}^\circ \quad 6$$

$$K_{s\alpha}^\circ = |A^{zA}| |B^{zB}|^{b(1-\alpha)} |C^{zC}|^{c\alpha}, \quad 7$$

where $|X|$ is the activity of X . Solubility Product Law (*i.e.* Mass Action Law for stoichiometric solids, Eq.7) is coming from terms $v_i d\xi$ in Eq.4; while for solid solutions the two terms of Eq.4 give two equations (see **¡Error! No se encuentra el origen de la referencia.**)

5.1 Solid solutions)

$$[A^{zA}] [B^{zB}]^{b(1-x)} [C^{zC}]^{cx} = K_{s0}^{1-x} K_{s1}^x (1-x)^{b(1-x)} x^{cx} \quad 8$$

$$[C^{zC}]^c / [B^{zB}]^b = (K_{s1}/K_{s0})^x (x^c / (1-x)^b) \quad 9$$

- which are also, by definition, the set of equations for ideal solid solutions, since in this cases activities are concentrations, *i.e.* in this case $K_i^\circ = K_i$.
- Eq.8 can as well be written $([A^{zA}][B^{zB}]^b)^{(1-x)} ([A^{zA}][C^{zC}]^c)^x = (K_{s0}(1-x)^b)^{1-x} (K_{s1} x^c)^x$, which was proposed by several authors.
- Eq.9 appears to be classical Mass Action Law for Equilibrium 5

Rearranging Eq.8 and 9 typically gives

$$[A^{zA}][B^{zB}]^b = K_{s0} (1-x)^b \quad 10$$

$$[A^{zA}][C^{zC}]^c = K_{s1} x^c, \quad 11$$

an equivalent set of equations, which are clearly Mass Action Law for A^{zA}/B^{zB} and A^{zA}/C^{zC} Ionic Exchange Equilibria. Since $0 < x < 1$ Eq.10 and 11 mean the end-members are not formed, when the ideal solid solution is stable: **ideal solid solutions are always stable** -however real solid solutions are not always observed, when this is not for kinetics reasons, this means they are not ideal- actually a consequence of how the stoichiometric coefficients were chosen *-i.e.* the way of splitting the solid solutions into two or more solid compounds of varying ratios-, intuitively this should respect actual ionic exchanges, and this is not predicted by Thermodynamics. Ideal solid solutions are always stable, is a consequence of a more general Thermodynamics properties of ideal systems

$$\Delta_{\text{mix}} G = G_x - G_2, \quad 12$$

the **mixing Gibbs energy** is always negative, where

$$G_x = \mu_{A_s} + b(1-x)\mu_{B_s} + c x \mu_{C_s} \quad 13$$

is the Gibbs Energy of the solid solution, and

$$G_2 = (1-x)G_0 + x G_1 \quad 14$$

is the Gibbs Energy, when the solid solution is not formed. Reporting $\mu_{x_s} = \mu_{x_s}^\# + R T \ln a_{x_s}$ in Eq.13 and 14, and since for consistency with Standard State, in endmembers activities are concentrations, Eq.12 writes

$$\Delta_{\text{mix}} G = R T \ln(|A_s^{zA}| |B_s^{zB}|/b)^{b(1-x)} (|C_s^{zC}|/c)^{cx} \quad 15$$

for ideal solid solutions $|A_s^{zA}| = 1$, $|B_s^{zB}| = b(1-x)$ and $|C_s^{zC}| = c x$

$$\Delta_{\text{mix}} G_{\text{id}} = R T \ln((1-x)^b x^{cx}) \quad 16$$



which is indeed negative, when the ideal solid solution is formed ($0 < x < 1$). This can equivalently be written as

$$\Delta_{\text{mix}}G_{\text{id}} = R T \ln([A^{\text{ZA}}] [B^{\text{ZB}}]^{b(1-x)} [C^{\text{ZC}}]^{cx} / (K_{\text{S0}}^{1-x} K_{\text{S1}}^x)) \quad 17$$

or

$$\Delta_{\text{mix}}G_{\text{id}} = R T \ln([B^{\text{ZB}}] / [B^{\text{ZB}}]_{\text{B}})^{b(1-x)} ([C^{\text{ZC}}] / [C^{\text{ZC}}]_{\text{C}})^{cx} \quad 18$$

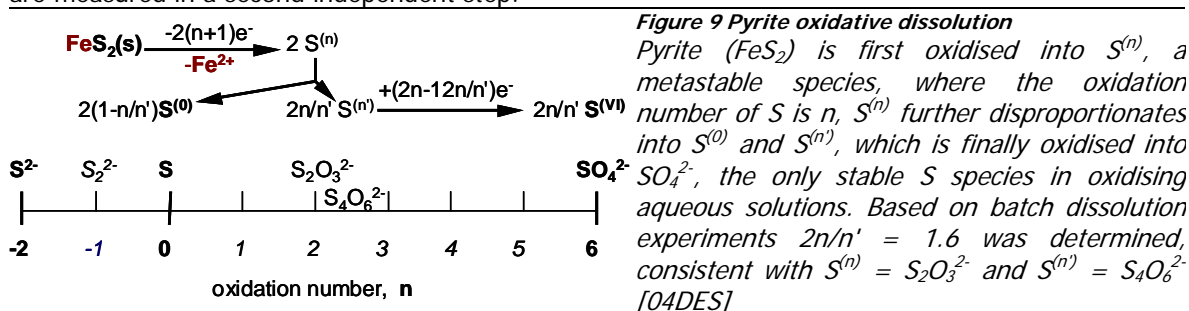
by comparing Eq.8 and 16, or by writing Eq.10 and 11 as $[A^{\text{ZA}}][B^{\text{ZB}}]^b = [A^{\text{ZA}}]_{\text{B}} [B^{\text{ZB}}]_{\text{B}}^b (1-x)^b$ and $[A^{\text{ZA}}][C^{\text{ZC}}]^c = [A^{\text{ZA}}]_{\text{C}} [C^{\text{ZC}}]_{\text{C}}^c K_{\text{S1}} x^c$, where $[X^{\text{ZX}}]_{\text{Y}}$ is X solubility as controlled by endmember $A\text{Y}_y(\text{s})$: $\Delta_{\text{mix}}G_{\text{id}}$ is linked to the decreases of $[B^{\text{ZB}}]$ and $[C^{\text{ZC}}]$ resulting from the formation of the solid solution.

Actually the thermodynamic calculation is the same for **liquid or surface ionic exchangers**, which is a theoretical way to identify their reference state with the usual standard state. Typically for ionic exchange sorption reactions (as typically Eq.5), equilibrium constant K is often measured, it can be interpreted as $K = K_{\text{S1}}/K_{\text{S0}}$ (Eq.9), specially when K_{S0} , the solubility product of the pure matrix is known: K_{S1} is deduced as $K_{\text{S1}} = K K_{\text{S0}}$, however K_{S1} can very well be for a surface precipitate.

2.5 Surface complexation formulas

We outlined above formula for calculating activity coefficients. Surface complexation formula are very popular in literature for modelling sorption. In this section we essentially point out both formula are based on similar physical models.

For calculating D, the Debye-Hückel term in γ_i , the activity coefficient for ion i, of charge z_i , Boltzmann and Poisson equations are solved in spherical geometry. One obtains ψ , the total electrostatic potential generated by z_i and its counter-ion atmosphere. ψ_i is subtracted from ψ , where ψ_i is the electrostatic potential generated only by Charge z_i , in vacuum. Surface complexation formula are based on Gouy and Chapman formula also obtained by solving Boltzmann and Poisson equations, but in planar semi-infinite geometry. However it seems ψ -not $\psi - \psi_i$ - was used for obtaining surface complexation formulas, which also use a simpler form for D, and do not include fitted ion pair terms, despite it was recently suggested they are certainly important for modelling other surface properties [04PEL]. Surface complexation formulas often include many fitted parameters, that cannot easily be measured independently, this because chemical bonding (complex formation) –not only weak interactions- are often included in the fit, while this is not the case for Solution Chemistry, where equilibrium constants are measured at constant ionic strength I, and ΔG_y are measured in a second independent step.



It might be worthwhile to compare Boltzmann - Poisson calculations in both situations. To our knowledge this has not systematically be done, while it might be interesting introducing ion pair parameters in the surface complexation formulas, providing these formulas are changed for being consistent with the usual standard state of aqueous solutions, this needs treating independently chemical bonding (*i.e.* surface complexing) and non ideality (*i.e.* aqueous counter ion effects on surface complexes) as reflected by $\psi - \psi_i$ -not ψ -. Anyhow surface complexation formulas might not be specially needed, since Ion Exchange Theory reasonably well accounts for many experimental results. It is an Ion Exchange Model based on a thermodynamic approach for ideal systems, in most cases it requires fewer fitted parameters. As outlined above for solid solutions, it is also easier to link this type of models to the standard state, a problem also debated in literature for Surface Complexation Formulas.

3. GEOCHEMISTRY

Actinide solubilities are very low in reducing conditions, as typically in deep groundwaters. In groundwaters, reducing conditions are maintained by several natural minerals: typically oxidative dissolution of Pyrite, a mineral containing S(-I) and Fe(II), two elements in reduced forms (Figure 9).

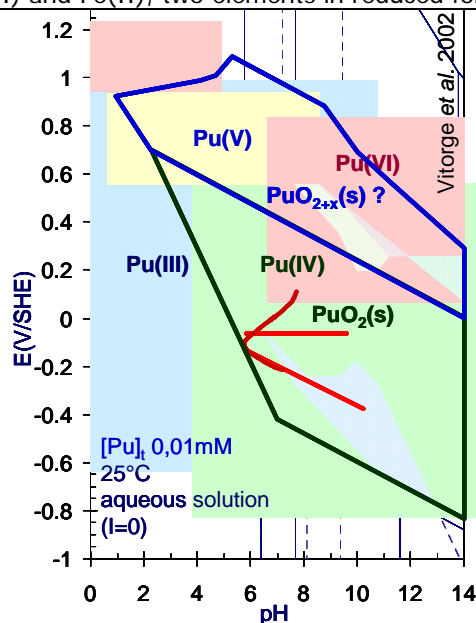


Figure 10: Pourbaix diagramme for Pu
 For clarity, the details of the soluble species at the same oxidation state are not written on this figure (coloured domains Pu(III), Pu(IV), Pu(V) and Pu(VI)). Bolded lines are for solid compounds $PuO_2(s)$ or $PuO_{2+x}(s)$. The stability of $PuO_{2+x}(s)$ was estimated by analogy assuming $MO_{2+x}(s)$ compounds include M^{4+} and MO_2^{2+} ions for $M = U$ or Pu ; however, for $x \leq 0.5$ they could as well be formed with MO_2^+ instead of MO_2^{2+} , which would increase the stability domains of $PuO_{2+x}(s)$ decreasing the domain of $PuO_2(s)$, since Pu(V) is more stable than U(V) (Figure 11a, [02VIT]). The red straight lines represent a part of a Pourbaix diagram near an U ore. The red bolded curve models oxidising waters arriving on the U ore. The dashed domains represent the influence of carbonate complexes (at $P_{CO_2} = 0.01$ atm) on the aqueous speciation of Pu: this would typically reduce the domain of Pu(IV), however this might merely reflect missing complexing data for Pu(IV).

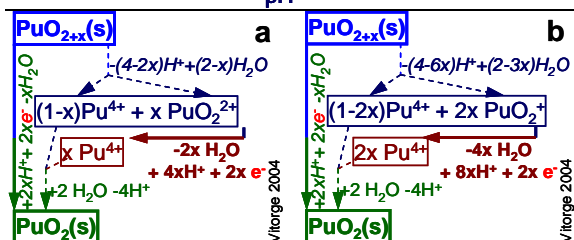


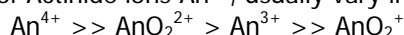
Figure 11: Estimating the stability of $PuO_{2+x}(s)$ by using analogies (dashed lines) for non-redox reactions [03VIT], assuming MO_2^{2+} (Figure 10 and Figure 11a) or MO_2^+ (Figure 11b) in MO_{2+x} .

When waste disposal studies started -in the early eighties- few and contradictory equilibrium constants and standard potentials of redox couples were published. We reinterpreted most of the publications on redox hydrolysis and carbonate complexation of actinides [01LEM, 95VIT, 98VIT, 99VIT and 03VIT] within the framework of the **NEA-TDB project**, the Thermochemical Data Base of the Nuclear Energy Agency (OECD), that produced selected thermodynamic data on U [92GRE], Am [95SIL], Tc [99RAR], and Np and Pu [01LEM]. TDB did not select any data, when the quality of the published experimental results was not high enough, even when reasonable estimates are possible. However for redox and hydrolysis reactions of U, Np, Pu and Am we extracted a more operational data base from the NEA-TDB tables and their comments [03VIT], and typically plotted Pourbaix diagrams for Pu, estimating by analogy possible stabilities of PuO_{2+x} (Figure 10).

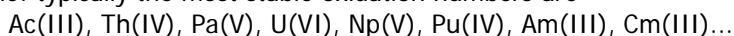
Chemical analogies are based on classical qualitative chemical rules. Many species dissolved in water are ions of oxidation states predicted by their position in Mendeleev Table: in the first columns the most stable oxidation number is the number of the column, typically Cs^+ , Sr^{2+} , Th^{4+} , $Pa(V)$, $U(VI)$ and $Tc(VII)$ hydrolysed as UO_2^{2+} and TcO_4^- respectively, radionuclides important for waste management. However, transition elements can be stable at lower oxidation states: U^{4+} can typically be stable in reducing conditions. f-transition elements of same charge are also chemical analogues as typically La^{3+} , U^{3+} , Np^{3+} , Pu^{3+} , Am^{3+} , Cm^{3+} ... Transuranien elements form stable aqua cations - in the order of the most to the less stable oxidation state-: $Np(V)$ (as NpO_2^+) > Np^{4+} > $Np(VI)$ (as NpO_2^{2+}) > Np^{3+} , $Pu^{4+} \geq Pu(V)$ (as PuO_2^+) > Pu^{3+} > $Pu(VI)$ (as PuO_2^{2+}), $Am^{3+} >> Am(V)$ (as AmO_2^+), Cm^{3+} ... All these **Actinide ions**



are hard cations [63PEA, 73 PEA and 93PEA], *i.e.* they have strong interactions with hard anions or electronegative donor atoms of neutral molecules, typically in ground waters H_2O , CO_3^{2-} , OH^- ... This hard/soft concept is a qualitative guideline; however, treating hard ions as hard charged spheres is a too rough approximation for quantitative molecular modelling [02DER, 03CLA]. Moreover, covalent bonding typically explains the differences in geometries between the iso-electronic UO_2^{2+} and ThO_2 molecules [81WAD]. This is certainly at the origin of the **Pa(V) exception**, the actinide element between Th and U in Mendeleev Table: in contrast with linear UO_2^+ , NpO_2^+ , PuO_2^+ and AmO_2^+ ions, PaO_2^+ is not stable in acidic media. Beside this exception, **Actinide ions at the same oxidation state are chemical analogues, and are chemical analogues of hard cations of similar Ratio z/r** , where z is the charge of the cation and r its ionic radius. For this reason it is usually enough to study one analogue, making only verifications for the other ones. The chemical reactivities of Actinide ions An^{z+} , usually vary in the order:



There ionic radii and mobilities vary in the reverse order; we indeed calculated the (NBO) charge of U in UO_2^{2+} is 3 or a little more (Figure 14). Conversely, charge transfers vary a lot within the actinide series as expected from their position in Mendeleev Table: typically the most stable oxidation numbers are



however charge transfers are involved (by definition) in redox reactions; but intra-molecular charge transfers are not much involved in most bonding for complexes of hard ions (by definition of hard ions), again this is only a thumb rule, since it seems very strong electrostatic interactions can also result in charge transfers as typically in NpO_2^+ , UO_2^{2+} , $\text{UF}_6(\text{g})$ quite covalent species *i.e.* electrostatic interactions can be enough (*vs.* temperature random energy) to form ionic complexes in aqueous solutions, while stronger interactions would enough decrease chemical bounds lengths for allowing stabilizing charge transfer, which also contributes to shortening chemical bounds. However, electrostatic reasoning is often enough for understanding chemical reactivity of hard ions, and when using analogies for estimating their missing data.

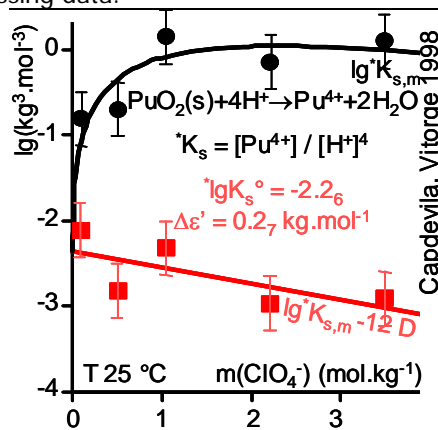


Figure 12: Standard solubility product of $\text{PuO}_2(\text{s})$. $[\text{Pu}^{4+}]$ was obtained by using an experimental set up equivalent to a specific Pu^{4+} electrode based on Pu(V) Disproportionation Equilibrium $2 \text{PuO}_2^+ \rightarrow \text{PuO}_2^{2+} + \text{PuO}_2(\text{s})$ at $-\lg[\text{H}^+] \approx 1$, where $[\text{PuO}_2^+]$ and $[\text{PuO}_2^{2+}]$ were measured by spectrophotometry [91CAP, 92CAP, 92CAP/VIT, 95CAP and 98CAP]. E , the redox potential of the solution was calculated from the measured ratio $[\text{PuO}_2^{2+}]/[\text{PuO}_2^+]$ and $E_{\text{PuO}_2^{2+}/\text{PuO}_2^+}$, the formal potential of the $\text{PuO}_2^{2+}/\text{PuO}_2^+$ redox couple measured independently by cyclic voltametry. Similarly from $[\text{Pu}^{3+}]$ (also measured by spectrophotometry) and $E_{\text{Pu}^{4+}/\text{Pu}^{3+}}$, $[\text{Pu}^{4+}]$ was obtained, from which *K_s was calculated, and extrapolated to $I = 0$ (Figure 4).

Typically for Actinides at oxidation state +4 An(IV) , the solubility is very low in a wide domain of pH values, and solubility measurements are practically the only direct experimental technique for determining aqueous speciation; unfortunately An(IV) oxides or hydroxides are ill defined, when obtained by precipitation in aqueous solution, *i.e.* at relatively low temperature. Nevertheless we could extract thermodynamic data from such experimental studies for Pu [98CAP, 99RAI and 03 VIT], despite Pu(IV) disproportionates in the chemical conditions, where many published experimental studies were performed for measuring *K_s , the solubility product of $\text{PuO}_2(\text{s})$. However, we took advantage of these disproportionation reactions for measuring *K_s (Figure 12).

4. MOLECULAR MODELING

Gibbs energies of reactions ($\Delta_r G = -R T \ln K$) are needed for predicting equilibrium aqueous speciation at constant temperature and pressure. Despite considerable efforts are currently devoted for developing methodologies and



computer programs based on Quantum Mechanics or Statistical Physics, it is still not clear, whether atomistic modelling can provide reliable numerical values for $\Delta_r G$'s in aqueous solutions, since $\Delta_r G$ is quite a small fraction of the total energy ab initio calculated. Ab initio calculations provide energies and optimised geometry in gas phase; atomic charges in molecules and some of the temperature contributions to the energy can also be estimated. This is at least a quantitative support for checking usual intuitive descriptions of chemical bonding and reactivity, as outlined here for hydrolysis of hard cations.

Ab initio and DFT calculations are typically used in literature for studying hydrated cations $[M(H_2O)_n]^{z+}$, usually limited to the first hydration shell, which is, indeed, the "simplest" M system in aqueous chemistry. However, we are interested in $ML_i^{z-i}L^-(aq)$, complexes with ligands L^- : in the first hydration shell H_2O 's are substituted by L^- 's. The simplest ligand is $L^- = OH^-$, which, anyhow, needs to be studied, since most actinide cations are hydrolysed in neutral conditions of environmental waters. Be^{2+} is a hard cation, quite analogue to UO_2^{2+} for first hydrolysis, and even for polynuclear hydrolysed species (Figure 13). Be is a light element which simplify ab initio calculations. Its first hydration shell is limited to $n \leq 4$, which limit the number of species to be calculated. We reproduced published ab initio calculations for the system Be^{2+}/H_2O , and it was even easier to calculate clusters, where $n H^+$'s were suppressed corresponding to System $Be^{2+}/H_2O/OH^-$. However this was not enough to obtain realistic estimations of numerical values for $\Delta_r G$ in liquid water at 298.15 K [00VIT]. The solvent can be modelled as a dielectric continuum; however this would not take into account water polymers modified *-i.e.* destroyed or stabilised- by an hydrated cation, which might very well be needed for such modelling.

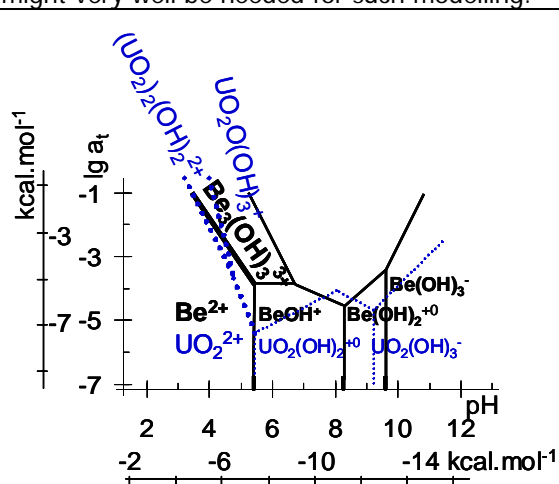


Figure 13: Hydrolysis of Be^{2+} and UO_2^{2+} . Predominance domains (\log_{10} of M total activity vs. pH) are drawn for $M^{2+} = Be^{2+}$ (bolded) and UO_2^{2+} (blue dotted lines) in liquid water (zero ionic strength) at 25°C, ignoring precipitation for clarity (polynuclear species form in nearly oversaturated to oversaturated solutions). Molar concentrations c_i ($mol.L^{-1}$) -here equal to activities ($mol.kg^{-1}$)- scales are related to energy ($kcal.mol^{-1}$) scales through chemical potentials $\mu_i = \mu_i^\circ + RT \ln c_i$. Smaller characters and thin lines are to stress relatively large uncertainties for the formation constants of the corresponding species. First hydrolysis (vertical line at about $pH = 5.2$), and the formations of the trinuclear species are observed in quite similar chemical conditions for both elements.

Nevertheless, we started a similar study on System $UO_2^{2+}/H_2O/OH^-$. We calculated several geometries for typically $UO_2(OH)_2(H_2O)_2$, while only one geometry was obtained for $UO_2OH(H_2O)_3^+$ (Figure 14). Many ab initio studies focus on the geometry of minimum energy, while we are rather interested in the Gibbs energy for the Systems including all possible geometries, intuitively the most stable species and those of energies higher by about kT (or RT for 1 mole). The total energy can be deduced from the partition function with usual approximations. The total energy is the mean energy on each geometry weighted by a Boltzmann factor, however, it is also stabilised by configurational entropy (see **¡Error! No se encuentra el origen de la referencia.**

5.2 Gibbs energy for several conformations), assuming Species A, actually correspond to several A_i , species of same stoichiometry:

$$G = G^\# + G_c \quad 19$$

where

$$G^\# = \sum_i (n_i G_i^\#) \quad 20$$

is the mean of $G_i^\#$ values weighted by

$$n_i = (e^{-(G_i^\# - G_0^\#)/RT}) / (\sum_i (e^{-(G_i^\# - G_0^\#)/RT})) \quad 21$$



the fraction of moles of Species A_i ; $G_i^\#$ is the Gibbs energy for 1 mole of species A_i alone. When A_0 is the most stable geometry, n_i appears to be Boltzmann factor.

$$G_c = \sum_i (n_i RT \ln n_i) \quad 22$$

is the mixing term. For close $G_i^\#$ values, *i.e.* $G = G_i^\#$ for any i , $n_i = 1/n$,

$$G_c = -RT \ln n \quad 23$$

where n is the number of conformers of similar energies, which gives the order of magnitude of G_c : at 25°C $RT \ln 10 = 5.7 \text{ kJ.mol}^{-1}$ corresponding to 1 order of magnitude on Equilibrium Constant K , or equivalently 1 \log_{10} unit on $\text{p}K_a$. This is not negligible as compared to the length of stability domains of aqueous species, typically the stability domain of UO_2OH^+ or AmOH^{2+} is quite smaller than the stability domain of $\text{UO}_2(\text{OH})_2(\text{aq})$ or $\text{Am}(\text{OH})_2^+$ respectively: for the later ones several conformers can be imagined (Figure 14).

However successive hydrolysis might very well be associated with changing coordination number, typically for U(VI) the most hydrated species in gas phase is certainly $\text{UO}_2(\text{H}_2\text{O})_5^{2+}$ taking into account only the first hydration shell, while its first hydrolysis species might very well be a mixture of $\text{UO}_2\text{OH}(\text{H}_2\text{O})_3^+$ and $\text{UO}_2\text{OH}(\text{H}_2\text{O})_4^+$ (Figure 14), with this rough models the first hydrolysis reaction is associated with the lost of 0 or 1 H_2O molecule: corresponding $G_{\text{H}_2\text{O}}$ is certainly more important than G_c . A realistic model for liquid water might very well need several $\text{M}(\text{H}_2\text{O})_i^{z+}$ species -*i.e.* several i values for any cation M^{z+} - which formally gives similar supplementary G terms; however, again $G_{\text{H}_2\text{O}}$ terms are certainly more important. This stresses it is of interest to determine the relevant number of water molecules for each hydrolysis species.

Various criteria are commonly -even implicitly- used in literature, we now will point out mass spectrometry results can give experimental information on this problem; however, this needs correct interpretation since we will see **hydration numbers determined by mass spectrometry** might be smaller than actual hydration numbers in aqueous solutions, because the activity of water is much smaller in mass spectrometers, than in liquid water. Moreover, mass spectrometry has also been extensively used for checking ab initio calculations of ions in vacuum. Gresham et al. produced M^+ ions by bombarding UO_3 in an IT-SIMS for $\text{M}^+ = \text{UO}(\text{OH})^+$, UO_2^+ and $\text{UO}_2(\text{OH})^+$, where Uranium is at oxidation states 4, 5 and 6 respectively [03GRE]. Each ion was selected for further reactions, which produced the hydrates at controlled water partial pressure of typically 1.2 to $1.4 \cdot 10^{-6}$ Torr. They interpreted their observations with Reactions



where $n = 0, 1, 2, 3$ and 4 for U(IV) and U(V), and $n = 0, 1, 2$ and 3 for U(VI). $\text{M}(\text{H}_2\text{O})_3^+$ ions were the major products after about 0.9, 0.4 and 1.2 second respectively for U(IV), U(V) and U(VI) respectively. For U(V), after about 1.4 second $\text{UO}_2(\text{H}_2\text{O})_4^+$ had about the same concentration as $\text{UO}_2(\text{H}_2\text{O})_3^+$. The authors modelled the kinetic curves with Reactions 24, and fitted the corresponding forward and reverse kinetic constants. This interpretation seems reasonable; despite there possibly were too many fitted parameters for allowing sensitivity analysis. Nevertheless, we estimated equilibrium constants

$$K_{n+1} = [\text{M}(\text{H}_2\text{O})_{n+1}^+] / ([\text{M}(\text{H}_2\text{O})_n^+] P_{\text{H}_2\text{O}}) \quad 25$$

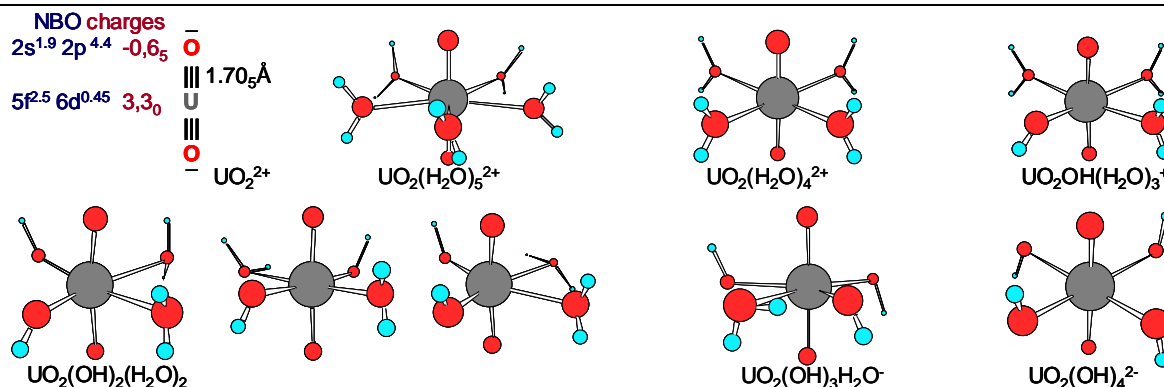


Figure 14: Ab initio optimised geometries of hydrated and hydrolysed UO₂²⁺ species

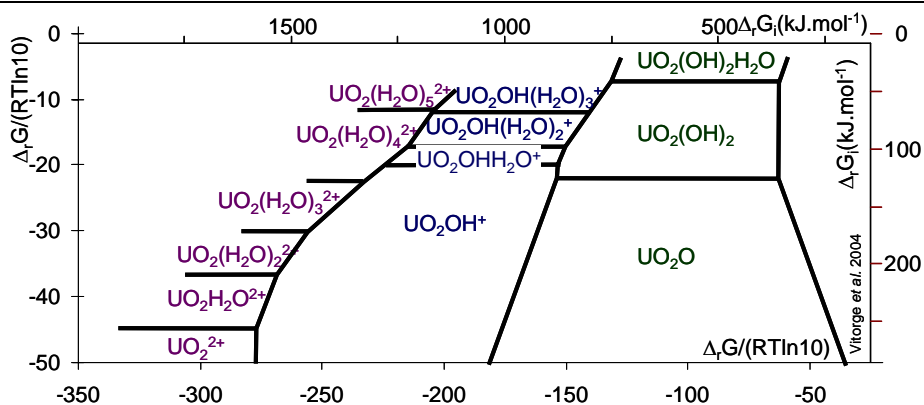


Figure 15 Hydration and hydrolysis Gibbs energy of U(VI)

The horizontal lines indicate $\Delta_r G$, the Gibbs energies (kJ.mol^{-1}) of Reactions 24 calculated at level B3LYP (in gas phase) with the suite of softwares Gaussian98 [98GAU] at 25°C for the most stable species of each stoichiometry (i.e. non including conformation energy). $\Delta_r G/(RT \ln 10)$ is \log_{10} of the corresponding equilibrium constant: it is interpreted as $\lg P_{\text{H}_2\text{O}^{1/2}}$, the \log_{10} of the H₂O partial pressure (atm) for the half point reaction, which is the frontier of the predominance domains of UO₂(OH)_i(H₂O)_{n-1}²⁻ⁱ and UO₂(OH)_i(H₂O)_n²⁻ⁱ species. The upper limit of the diagram correspond to Reaction H₂O(g) → H₂O(l). Similarly the vertical lines are for Reactions UO₂(OH)_{i-1}(H₂O)_n³⁻ⁱ + OH → UO₂(OH)_i(H₂O)_n²⁻ⁱ. UO₂O(H₂O) and UO₂(OH)₂ typically have the same stoichiometry, however the later geometry in the most stable.

as the ratios of the forward / reverse kinetic constants (**¡Error! No se encuentra el origen de la referencia.**

5.3 Treatment of mass spectrometry data from Ref.[03gre]). $1/K_{n+1}$ can be interpreted as $P_{(\text{H}_2\text{O})_{1/2, n+1}}$, the H₂O partial pressure at the half point reaction -i.e. for $[\text{M}(\text{H}_2\text{O})_{n+1}^+] = [\text{M}(\text{H}_2\text{O})_n^+]$ - a classical interpretation used for solution chemistry. However the unit conversions (they are in **¡Error! No se encuentra el origen de la referencia.**

5.3 Treatment of mass spectrometry data from Ref.[03gre]) depends on temperature, while it is not clear whether thermal equilibrium was achieved: this is certainly the reason why the authors did not write this type of interpretation.

The values we calculated for $P_{(\text{H}_2\text{O})_{1/2, n}}$ are all in the range $10^{-9.8} - 10^{-7.8}$ atm, this would apparently mean the intermediary species would not be much stable; however, as discussed just below, this is rather originated in kinetics control of first hydration reactions, while only the higher hydrated species were in equilibrium conditions, or close to.

$10^{-9.8} - 10^{-7.8}$ atm, the values we calculated for $P_{(\text{H}_2\text{O})_{1/2, n}}$ are close to $10^{-8.8}$ atm, the experimental $P_{\text{H}_2\text{O}}$ in the mass spectrometer (Table 2). Our calculations relied on several assumptions; but it seems the most important one, is a



constant value for each K_n during each experiment, as a consequence of constant values for the experimental kinetic constants. This was not specially expected since K_n is a (actually thermodynamic) constant at constant pressure and temperature, while the relevant experimental temperature is difficult to estimate and was even probably not defined at short times. The intermediary species were rather produced at the beginning of the experimental observations, while the major species were rather produced at the end. For this reason, the corresponding relevant temperatures might be different for the different species, *i.e.* for their calculated characteristic $P_{(H_2O)_{1/2},n}$ values. Gresham et al. did not produced any sensitivity analysis of their model, however the shapes of the experimental curves for the intermediary species, might very well accommodate models with non-constant kinetic "constants". Anyhow, since the calculated $P_{(H_2O)_{1/2},n}$ values are of the order of magnitude of the experimental P_{H_2O} values, this is an indication that they are indeed estimations of the minimal P_{H_2O} value required to form the final products: $UO(OH)(H_2O)_3^+$, $UO_2(H_2O)_3^+$, $UO_2(H_2O)_4^+$ and $UO_2(OH)H_2O_3^+$. Higher hydrates would probably form at higher P_{H_2O} value. This also means this technique does not necessarily provide the numbers of water molecules in the first hydration shells of hydrated cations in liquid water.

$\Delta_r G$ calculated *ab initio* also indicate $UO_2(OH)H_2O_3^+$ is the most stable U(VI) monocation at $10^{-8.8}$ atm (Figure 15). These calculations also indicate the maximum number of water molecules in the first hydration shell might be limited by the activity of water, and not always by steric considerations.

5. APPENDIX

5.1 Solid solutions

In this Appendix we indicate some details of the calculations given in the above text.

$$\Delta_r G_{s\alpha}^\circ = \mu_A^\circ + b(1-\alpha)\mu_B^\circ + c x \mu_C^\circ \quad 26$$

where μ_X° is the standard chemical potential of X^{zX} , an aqueous ion, and $|X^{zX}|$ its activity, here superscript $^\circ$ means in the standard state, *i.e.* activities are used, not concentrations. When x varies, term $\int v_i' dx$ in Eq.4 generate another set of equations. However at constant $x = \alpha$, μ_{X_s} 's were constant, included in equilibrium constant $K_{s\alpha}$, where μ_{X_s} is the chemical potential of Ion X^{zX} in the solid. Introducing $\delta_X = \mu_X - \mu_{X_s}$, the two sets of equations for solid solutions are

$$\Delta_r G_x^\# = -RT \ln K_x^\# \quad 27$$

$$\Delta_r G_x^\# = \delta_A^\# + b(1-x)\delta_B^\# + cx \delta_C^\# \quad 28$$

$$K_x^\# = \frac{|A^{zA}|^a |A_s^{zA}|^b}{(|B^{zB}|^b |B_s^{zB}|)^{b(1-x)} (|C^{zC}|^c |C_s^{zC}|)^{cx}} \quad 29$$

and

$$\Delta_r G_{BC}^\# = -RT \ln K_{BC}^\# \quad 30$$

$$\Delta_r G_{BC}^\# = -b \delta_B^\# + c \delta_C^\# \quad 31$$

$$K_{BC}^\# = \frac{|C^{zC}|^c |B_s^{zB}|^b}{(|B^{zB}|^b |C_s^{zC}|)^c} \quad 32$$

Now superscript $^\#$ means in a reference state, which is not the standard state, namely $\mu_A^\# = \mu_A^\circ$, $\mu_B^\# = \mu_B^\circ$, $\mu_C^\# = \mu_C^\circ$, $\mu_{A_s}^\# = \mu_{A_s}^\circ = \mu_{B_s}^\circ = \mu_{B_s}^\circ = 0$, but $\mu_{B_s}^\# = -RT \ln \chi_{B_s}^\circ$ and $\mu_{C_s}^\# = -RT \ln \chi_{C_s}^\circ$. For convenience, we use the following concentrations in the solid: $\chi_{A_s} = 1$, $\chi_{B_s} = b(1-x)$ and $\chi_{C_s} = cx$, and $\chi_{B_s}^\circ = b$ and $\chi_{C_s}^\circ = c$. For concentration units, we chose ratios n_x/n_A , which is not exactly the usual mole fraction, thermodynamics does not indicate which units and notations should be chosen for concentrations and stoichiometric coefficients, however, concentrations must be intensive variables, and their unity is linked to the definition of the reference state.

Eq.32 is a classical form of mass action law for Eq.5, a classical equilibrium *-i.e.* with constant stoichiometric coefficients. However, neither $\Delta_r G_x$, nor K_x are constant. Equivalent sets of equations were already established [O2MIC], we only clarified that both sets of equations must be solved simultaneously: for ideal solid solutions this is enough to calculate aqueous and solid speciations. These equations had been obtained by identifying standard states, *i.e.* for endmembers, where $x = 0$ or 1 respectively, Solubility is the same, when calculated as for stoichiometric



(Eq.7) or non-stoichiometric (Eq.29) compounds. For this the following linear combination can also be used

$$\Delta_r G_x = (1-x)\Delta_r G_0 + x \Delta_r G_1 \quad 33$$

$$\Delta_r G_{BC} = \Delta_r G_1 - \Delta_r G_0 \quad 34$$

By definition the endmembers are ideal, *i.e.* $|A_s^{zA}| = 1$, $|B_s^{zB}| = b(1-x)$ and $|C_s^{zC}| = c x$ for $x = 0$ and 1 : $K_{s0} = K_0 b^b$ and $K_{s1} = K_1 c^c$. The stoichiometric coefficients are also the concentrations in the solid solution. Finally, including the activity coefficients in the equilibrium constants, the **working equations** are:

$$[A^{zA}] [B^{zB}]^{b(1-x)} [C^{zC}]^{cx} = K_{s0}^{1-x} K_{s1}^x (1-x)^{b(1-x)} x^{cx} \quad 8$$

$$[C^{zC}]^c / [B^{zB}]^b = (K_{s1}/K_{s0}) (x^c / (1-x)^b) \quad 9$$

5.2 Gibbs energy for several conformations

Soluble species are often stable with different geometries of similar energies, namely species A actually corresponds to different geometries $A_0, A_1 \dots A_{n-1}$. The stability of A is given by its Gibbs energy

$$G = \sum_i n_i G_i \quad 35$$

where G_i is the Gibbs energy of A_i as typically ab initio calculated.

$$K_i = [A_i]/[A_0] \quad 36$$

is the equilibrium constant for Reaction



where

$$\Delta_r G_i = -RT \ln K_i = G_i^\# - G_1^\# \quad 38$$

$[A_i]$ ($=n_i/V$, where V is the volume of the system) is the concentration of A_i , similarly its partial pressure could be used for calculations in gas phase. $G_i^\#$ is G_i value in the reference state, for convenience we chose it as 1 mol of hypothetical pure A_i . $G_i^\#$ is typically given by usual ab initio softwares, when calculating frequencies after a geometry optimisation. For a system of 1 mol of A

$$1 = \sum_i n_i \quad 39$$

$$G_i = G_i^\# + R T \ln n_i \quad 40$$

where R ($= k N_A$, where k is Boltzmann constant, and N_A is Avogadro number) is the gas constant, n_i is the number of mol of A_i , rearranging the above equations for ideal systems $K_i = n_i/n_0 = e^{-(G_i^\# - G_0^\#)/RT}$,

$$1 = n_0 \sum_i (e^{-(G_i^\# - G_0)/RT}) \quad 41$$

$$G = n_0 \sum_i (e^{-(G_i^\# - G_0)/RT} (G_i^\# + RT \ln n_i)) \quad 42$$

which is rearranged as

$$G = G^\# + G_c \quad 19$$

where

$$G^\# = \sum_i (n_i G_i^\#) \quad 20$$

appears to be the mean value of $G_i^\#$ values weighted by n_i , where $G_i^\#$ is the G_i value for hypothetical pure A_i , and

$$n_i = (e^{-(G_i^\# - G_0^\#)/RT}) / (\sum_i (e^{-(G_i^\# - G_0)/RT})) \quad 21$$

is the Boltzmann factor when choosing the most stable geometry as A_0 .

$$G_c = \sum_i (n_i RT \ln n_i) \quad 22$$

appears to be a mixing term. Typically for 2 species, $n_0 = x$ and $n_1 = 1-x$, G_c is similar to $\Delta_{\text{mix}} G_{\text{id}}$ (Eq.16).

5.3 Treatment of mass spectrometry data from Ref.[03gre]

Gresham *et al.* provided numerical values for k_{forward} ($\text{cm}^3 \cdot \text{molecule}^{-1} \cdot \text{s}^{-1}$), the kinetic constants for reaction



and k_{reverse} (s^{-1})s for the reverse reaction. We assumed their definition were

$$k_{\text{forward}} \{M(\text{H}_2\text{O})_n^+\} c\{\text{H}_2\text{O}\} dt = -d\{M(\text{H}_2\text{O})_n^+\}$$

$$k_{\text{reverse}} \{M(\text{H}_2\text{O})_{n+1}^+\} dt = d\{M(\text{H}_2\text{O})_n^+\}$$

where $\{X\}$ is X concentration ($\text{molecule} \cdot \text{cm}^{-3}$); however, more usual macroscopic concentration units are ($\text{mol} \cdot \text{L}^{-1}$), we calculated

$$k_f = 10^{-3} N_A k_{\text{forward}} (\text{L} \cdot \text{mol}^{-1} \cdot \text{s}^{-1})$$



$$k_f = k_{\text{reverse}}(s^{-1})$$

$$k_f/k_r = [M(H_2O)_{n+1}^+] / ([M(H_2O)_n^+][H_2O]) = K$$

is the constant of Equilibrium 24. At half reaction (*i.e.* for $[M(H_2O)_{n+1}^+] = [M(H_2O)_n^+]$)

$$[H_2O]_{1/2} = 1/K. = (1000/N_A)k_{\text{reverse}}/k_{\text{forward}}$$

Since pressures were low $P_{(H_2O)_{1/2}}$, the corresponding water pressure can be calculated by using $PV = nRT$, where n/V and P units are mol.m^{-3} (*i.e.* $10^{-3} \text{ mol.L}^{-1}$) and Newton.m^{-2} (*i.e.* $1/101325 \text{ atm}$) respectively:

$$P_{(H_2O)_{1/2}} = (1000 [H_2O]_{1/2}/101325)RT$$

$$= 10^6 R T k_{\text{reverse}}/(101325 N_A k_{\text{forward}})$$

Using the values of the following table

N_A	6.02213 ₆₇	10^{23} mol^{-1}
R	8.3145 ₁₀	$\text{J.K}^{-1}.\text{mol}^{-1}$
T	298.15	K
$R T$	2.4789 ₇₁	kJ.mol^{-1}
$R T \ln 10$	5.7080 ₄₂	kJ.mol^{-1}
$\text{Pa}^\circ = 1 \text{ atm}$	101325	$\text{Pa} (= \text{Newton.m}^{-2})$
$10^6 R T / (\text{Pa}^\circ N_A)$	4.0626	10^{-20}
	$= 10^{-19.3912}$	

$$\lg P_{(H_2O)_{1/2}} = -19.39 + \lg(k_{\text{reverse}}/k_{\text{forward}})$$

Experimental water partial pressures P , were given in Torr, for comparison, we calculated

$$\lg P_{H_2O}(\text{atm}) = \lg P - \lg(760) = \lg P - 2.8808.$$



Table 2 Fitted kinetic constants to model IT-SIMS experimental observations for hydrates of U(IV), U(V) and U(VI) monocations [03GRE].

k_{forward} and k_{reverse} are the kinetic constants fitted in Ref.[03GRE] for Reactions 24, the $P_{\text{H}_2\text{O}}$ values are also given in Ref.[03GRE]. $P_{(\text{H}_2\text{O})_{1/2}}$ is calculated from the kinetic constants (see text)*.

		k_{forward} ($\text{cm}^3 \cdot$ molecule ⁻¹ $\cdot \text{s}^{-1}$)	k_{reverse} (s^{-1})	$P_{\text{H}_2\text{O}}$ (Torr)	$\lg P_{(\text{H}_2\text{O})_{1/2}}$ ($\lg(\text{atm})$)	$\lg(P_{\text{H}_2\text{O}})$ ($\lg(\text{atm})$)
2	$[\text{UOOH}]^+ + \text{H}_2\text{O} \leftarrow; \rightarrow [\text{UOOH}(\text{H}_2\text{O})]^+$	$8 \cdot 10^{-11}$	9	$1.4 \cdot 10^{-6}$	-8.3 ₄ *	-8.7 ₃
3	$[\text{UOOH}(\text{H}_2\text{O})]^+ + \text{H}_2\text{O} \leftarrow; \rightarrow [\text{UOOH}(\text{H}_2\text{O})_2]^+$	$2 \cdot 10^{-10}$	2		-9.3 ₉ *	
4	$[\text{UOOH}(\text{H}_2\text{O})_2]^+ + \text{H}_2\text{O} \leftarrow; \rightarrow [\text{UOOH}(\text{H}_2\text{O})_3]^+$	$3 \cdot 10^{-11}$	0.14		-9.7 ₂ *	
5	$[\text{UOOH}(\text{H}_2\text{O})_3]^+ + \text{H}_2\text{O} \leftarrow; \rightarrow [\text{UOOH}(\text{H}_2\text{O})_4]^+$	$3 \cdot 10^{-11}$	11		-7.8 ₃	
6	$[\text{UO}_2]^+ + \text{H}_2\text{O} \leftarrow; \rightarrow [\text{UO}_2(\text{H}_2\text{O})]^+$	$6 \cdot 10^{-11}$	8	$1.2 \cdot 10^{-6}$	-8.2 ₇ *	-8.8 ₀
7	$[\text{UO}_2(\text{H}_2\text{O})]^+ + \text{H}_2\text{O} \leftarrow; \rightarrow [\text{UO}_2(\text{H}_2\text{O})_2]^+$	$3 \cdot 10^{-10}$	15		-8.6 ₉ *	
8	$[\text{UO}_2(\text{H}_2\text{O})_2]^+ + \text{H}_2\text{O} \leftarrow; \rightarrow [\text{UO}_2(\text{H}_2\text{O})_3]^+$	$4 \cdot 10^{-10}$	2.2		-9.6 ₅ *	
9	$[\text{UO}_2(\text{H}_2\text{O})_3]^+ + \text{H}_2\text{O} \leftarrow; \rightarrow [\text{UO}_2(\text{H}_2\text{O})_4]^+$	$6 \cdot 10^{-11}$	1.7		-8.9 ₄	
10	$[\text{UO}_2\text{OH}]^+ + \text{H}_2\text{O} \leftarrow; \rightarrow [\text{UO}_2\text{OH}(\text{H}_2\text{O})]^+$	$4 \cdot 10^{-11}$	1	$1.4 \cdot 10^{-6}$	-8.9 ₉ *	-8.7 ₃
11	$[\text{UO}_2\text{OH}(\text{H}_2\text{O})]^+ + \text{H}_2\text{O} \leftarrow; \rightarrow [\text{UO}_2\text{OH}(\text{H}_2\text{O})_2]^+$	$1 \cdot 10^{-10}$	0.8		-9.4 ₈ *	
12	$[\text{UO}_2\text{OH}(\text{H}_2\text{O})_2]^+ + \text{H}_2\text{O} \leftarrow; \rightarrow [\text{UO}_2\text{OH}(\text{H}_2\text{O})_3]^+$	$5 \cdot 10^{-11}$	0.22		-9.7 ₅	

*Equilibrium constant K , is calculated as $k_{\text{forward}}/k_{\text{reverse}}$, with unit conversions its thermodynamics interpretation is $K = 1/P_{(\text{H}_2\text{O})_{1/2}}$ assuming equilibrium was achieved, which was certainly not for most species, excepted maybe for the most hydrated ones, namely Equilibria 5, 9 and 12.

Table 3 $\epsilon_{\text{Ln}^{3+}, \text{ClO}_4^-}$ - estimated from $\epsilon_{\text{Ln}^{3+}, \text{ClO}_4^-}$ values

See Figure 8

Ln	3/r	$\epsilon_{\text{Ln}^{3+}, \text{ClO}_4^-}$	An	3/r	$\epsilon_{\text{An}^{3+}, \text{ClO}_4^-}$
La	2,308	0,462	Ac	2,381	0,454
Ce	2,338	0,458	Th	2,459	0,46
Pr	2,370	0,454	Pa	2,542	0,487
Nd	2,402	0,454	U	2,575	0,492
Pm	2,433	0,458	Np	2,609	0,494
Sm	2,461	0,461	Pu	2,632	0,491
Eu	2,488	0,469	Am	2,691	0,499
Gd	2,515	0,476	Cm	2,703	0,5
Tb	2,542	0,487	Bk	2,727	0,503
Dy	2,571	0,493	Cf	2,752	0,506
Ho	2,597	0,490			
Er	2,622	0,493			
Tm	2,646	0,492			
Yb	2,667	0,495			
Lu	2,686	0,490			



Table 4 $\varepsilon_{M^{z+}, X^{z-}}$ values

$\varepsilon_{M^{z+}, X^{z-}}$ is calculated from $\lg \gamma_{\pm}$, the decimal log of the mean activity coefficient calculated from Pitzer coefficients (as explained for Figure 4), in $m = 4 \text{ mol.kg}^{-1}$ aqueous solutions, or for the maximum m values, where γ_{\pm} values are available. Uncertainty is the maximum value of $|\varepsilon(m) - \varepsilon(4)|$ for $0.5 < m < 4 \text{ mol.kg}^{-1}$, this only reflects the theoretical error of the SIT formula; however, it is virtually the total uncertainty on $\lg \gamma$ when calculated with this formula. Three digits are tabulated despite this is not meaningful, when compared with the uncertainty; however, this avoids propagating rounding errors in calculations, since SIT Formula can be used up to 4 mol.kg^{-1} for estimating $\lg \gamma = -Z^2 D + \varepsilon m$. The numerical values here tabulated reproduce isopiestic measurements with enough accuracy for speciation calculations; however, ε values can include possible weak complexing in the activity coefficient, for this reason, it would not be consistent to use these ε values with the corresponding complexing constant.

	NO_3^-	ClO_4^-	Cl^-		OH^-
Cd^{2+}		0.086±0.019			Li^+ -0.027±0.049
Pb^{2+}	-0.260±0.093	0.178±0.021			Na^+ 0.053±0.034
UO_2^{2+}	0.239±0.008	0.511±0.052	0.207±0.012		K^+ 0.094±0.018
Al^{3+}			0.376±0.002		Cs^+ 0.099±0.013
Sr^{3+}			0.317±0.002		
Y^{3+}	0.186±0.014		0.339±0.058		
La^{3+}	0.079±0.016	0.462±0.025	0.270±0.030		HSO_4^-
Ce^{3+}			0.249±0.006		Na^+ 0.014±0.009
					K^+ -
Pr^{3+}	0.082±0.010	0.454±0.022	0.282±0.039		0.039±0.042
Nd^{3+}	0.083±0.003	0.454±0.021	0.289±0.046		Mg^{2+} 0.333±0.045
Sm^{3+}	0.087±0.001	0.461±0.023	0.294±0.041		Ca^{2+} 0.123±0.051
Eu^{3+}	0.097±0.000		0.299±0.039		Fe^{2+} 0.380±0.111
Gd^{3+}	0.114±0.009	0.476±0.023	0.309±0.046		
Tb^{3+}	0.136±0.016	0.487±0.023	0.319±0.049		
Dy^{3+}	0.151±0.012	0.493±0.022	0.325±0.051		
Ho^{3+}	0.165±0.013	0.490±0.023	0.331±0.052		
Er^{3+}	0.183±0.021	0.493±0.022	0.336±0.061		
Tm^{3+}	0.193±0.021	0.492±0.020	0.339±0.065		
Yb^{3+}	0.197±0.017	0.495±0.023	0.343±0.069		
Lu^{3+}	0.199±0.010	0.490±0.019	0.343±0.070		
Cr^{3+}	0.285±0.008	-0.255±0.113	0.331±0.002		
Ga^{3+}		0.547±0.006			
Th^{4+}	0.160±0.020		0.350±0.013		

Table 4 $\epsilon Mz+$, $Xz-$ values (continued)

	NO_3^-	ClO_4^-	Cl^-	I^-	Br^-	F^-
H^+	0.060±0.012	0.142±0.033	0.125±0.016	0.185±0.019	0.157±0.007	
Li^+	0.077±0.005	0.148±0.008	0.109±0.019	0.155±0.004	0.106±0.009	
Na^+	-0.034±0.039	0.013±0.016	0.037±0.024	0.080±0.008	0.055±0.020	-0.039±0.012
K^+	-0.101±0.083		0.004±0.031	0.020±0.015	0.009±0.027	0.011±0.013
Rb^+	-0.104±0.097		-0.005±0.044	-0.009±0.049	-0.009±0.043	0.042±0.006
Cs^+	-0.176±0.039		-0.017±0.071	-0.041±0.061	-0.023±0.078	0.068±0.012
NH_4^+	-0.055±0.056	-0.110±0.034	0.000±0.031	0.011±0.002	-0.010±0.012	
Tl^+		-0.177±0.034				
Mg^{2+}	0.165±0.001	0.337±0.014	0.248±0.074	0.377±0.062	0.309±0.052	0.245±0.067
Ca^{2+}	0.017±0.010	0.266±0.005	0.194±0.053	0.262±0.006	0.197±0.006	0.142±0.007
Sr^{2+}	-0.051±0.012	0.223±0.004	0.160±0.052	0.237±0.008	0.164±0.001	0.163±0.047
Ba^{2+}		0.150±0.005		0.224±0.006	0.123±0.002	0.069±0.005
Mn^{2+}						0.122±0.008
Fe^{2+}						0.145±0.008
Co^{2+}	0.163±0.026			0.348±0.028	0.277±0.039	0.177±0.026
Ni^{2+}						0.196±0.045
Cu^{2+}	0.134±0.021					0.075±0.004
Zn^{2+}	0.162±0.005			0.299±0.021	0.175±0.044	0.015±0.031

Table 4 $\epsilon Mz+$, $Xz-$ values (continued)

	Li^+	Na^+	K^+	Rb^+	Cs^+	NH_4^+
ClO_3^-	0.0990.017	-0.0020.035				
BrO_3^-	0.0420.032	-0.0760.015				
SCN^-		0.0520.007	-0.0050.023			
NO_2^-	0.0730.005	0.0010.047	-0.0320.079	-0.0430.108	-0.0210.056	
HPO_4^-		-0.0720.090	-0.1760.042			-0.1250.182
HAsO_4^-		-0.0810.004	-0.1360.026			
SO_4^{2-}	0.0060.076	-0.0540.138		-0.1200.039	-0.0990.036	-0.0670.170
HPO_4^{2-}		-0.1670.030	-0.1210.036			
HAsO_4^{2-}		-0.1030.007	-0.0330.004			

Table 4 $\epsilon Mz+$, $Xz-$ values (continued)

	Na^+		K^+
HSe^-	-	PF_6^-	-
	0.015±0.007		0.292±0.059
B(OH)_4^-	-	Pt(CN)_4^{2-}	-
	0.047±0.091		0.005±0.035
BF_4^-	-	$\text{P}_3\text{O}_9^{3-}$	-
	0.054±0.045		0.002±0.008
CrO_4^{2-}	-	Fe(CN)_6^{3-}	-
	0.071±0.021		0.036±0.017
		Co(CN)_6^{3-}	-
			0.055±0.041
		Fe(CN)_6^{4-}	-
			0.139±0.016
		Mo(CN)_8^{4-}	-
			0.114±0.024



6. REFERENCE

- [63PEA] Pearson, R.G. (1963) J. Am. Chem. Soc. 85, 3533-3539
- [73PEA] Pearson, R.G. (1973) Hard and Soft Acids and Bases, Dowden, Hutchinson & Ross Inc, Stroudsburg, PA
- [81WAD] Wadt, W. (1981) J. Am. Chem. Soc., 103, p6053-6057
- [83MIC] Michard G. (1983) EUR 8590.
- [84VIT] Vitorge P. (1984) IAEA-SR-104/25
- [85COM] Côme B. (1985) EUR 9543
- [85KIM] Kim J. (1985) EUR 10023
- [86GRE] Grenthe I., Robouch P., Vitorge P. (1986) J. Less. Common Metals, 122, 225-231
- [87RIG] Riglet Ch., Vitorge P., Grenthe I. (1987) Inorg. Chim. Acta. 133, 2, 323-329
- [87ROB] Robouch P. (1987) PhD. Thesis Université Louis Pasteur, Strasbourg (France). CEA-R-5473
- [88WEA] Handbook
- [89RIG] Riglet Ch. (1989) PhD. Thesis Université Paris 6 (France). CEA-R-5535 (1990)
- [89RIG2] Riglet Ch., Robouch P., Vitorge P. (1989) Radiochim. Acta. 46, 2, 85-94
- [90CAP] Capdevila H., Vitorge P. (1990) J. Radioanal. and Nuclear Chem., Articles, 143, 2, 403-414
- [90GRI] Grimaud D., Beaucaire C., Michard G. (1990) Applied Geochemistry, Vol.5, 515-525
- [92CAP] Capdevila H. (1992) PhD. Thesis Université Paris-sud, Orsay (France) CEA-R-5643
- [92CAP2] Capdevila H., Vitorge P., Giffaut E. (1992) Radiochim. Acta 58/59, 1, 45-52
- [92GRE] Grenthe I., Fuger J., Konings R.J.M., Lemire R.J., Muller A.B., Nguyen-Trung C., Wanner H. (1992) Chemical thermodynamics of uranium. Paris OCDE AEN, Elsevier ed.
- Jensen S. (1982) EUR 7676
- [93PEA] Pearson R.G.; Chattaraj P.K., Parr R.G.; Gazquez J.L.; Komorowski L.; March N.H.; Sen K.D.; Politzer P., Murray J.S., Grice M.E; Nalewajski R. F.; Baekelandt B.G., Mortier W.J., Schoonheydt R. A.; Alonso J.A., Balbas L.C. (1993) Chemical Hardness. Structure and Bonding Volume 80. Sen K. D. Guest Editor Springer-Verlag Berlin 1993. ISBN 3-540-56091-2
- [94GIF] Giffaut E., Vitorge P., Capdevila H. (1994) J. Alloys Compounds 213/214, 278-285; also pre-published with supplementary materials as Giffaut E., Vitorge P., Capdevila H. (1993) CEA-N-2737.
- [95CAP] Capdevila H., Vitorge P. (1995) Radiochim. Acta 68, 1, 51-62. Prepublished with supplementary materials as CEA-N-2762 (1994)



[95SIL] Silva R. J., Bidoglio G., Rand M.H., Robouch P. B., Wanner H., Puigdomenech I. (1995), Chemical thermodynamics of americium. edited by Puigdomenech I., NEA OECD Elsevier ed.

[95VIT] Vitorge P. (1995) CEA-BIB-246.

[96CAP] Capdevila H., Vitorge P., Giffaut E., Delmau L. (1996) Radiochim. Acta 74, 93-98

[96TRO] Trotignon L., Beaucaire C., Louvat D., Aranyosy J.F. (1999) Applied Geochemistry, 14, 907-916.

[98GAU] Gaussian 98 (Revision A.9), M. J. Frisch, G. W. Trucks, H. B. Schlegel, G. E. Scuseria, M. A. Robb, J. R. Cheeseman, V. G. Zakrzewski, J. A. Montgomery, Jr., R. E. Stratmann, J. C. Burant, S. Dapprich, J. M. Millam, A. D. Daniels, K. N. Kudin, M. C. Strain, O. Farkas, J. Tomasi, V. Barone, M. Cossi, R. Cammi, B. Mennucci, C. Pomelli, C. Adamo, S. Clifford, J. Ochterski, G. A. Petersson, P. Y. Ayala, Q. Cui, K. Morokuma, D. K. Malick, A. D. Rabuck, K. Raghavachari, J. B. Foresman, J. Cioslowski, J. V. Ortiz, A. G. Baboul, B. B. Stefanov, G. Liu, A. Liashenko, P. Piskorz, I. Komaromi, R. Gomperts, R. L. Martin, D. J. Fox, T. Keith, M. A. Al-Laham, C. Y. Peng, A. Nanayakkara, C. Gonzalez, M. Challacombe, P. M. W. Gill, B. G. Johnson, W. Chen, M. W. Wong, J. L. Andres, M. Head-Gordon, E. S. Replogle and J. A. Pople, Gaussian, Inc., Pittsburgh PA, 1998.

[98RIG] Martial-Riglet C., Vitorge P, Calmon V. (1998) Radiochim. Acta 82, 69-76

[98VIT] Vitorge P., Capdevila H. (1998) CEA-R-5793

[99CAP] Capdevila H., Vitorge P. (1999) Czech. J. Phys. 49/S1, 603-609

[99RAR] Rard J.A., Rand M.H., Anderegg G., Wanner H. Chemical thermodynamics of technetium. (1999) OCDE NEA. Elsevier ed.

[99VIT] Vitorge P. (1999) Techniques de l'ingénieur, article B 3520. Formulaire form.B 3520.

[99VIT/BEA] Vitorge P., Beaucaire C., Fauré M.-H. , Maillard S., Capdevila H. (1999) Workshop on Solubility of actinides in relation with nuclear waste matrices. Mol (Belgium) 19-20/05/1999.

[00BEA] Beaucaire C., Pitsch H., Toulhoat P., Motellier S., Louvat D. (2000) Applied Geochem. 15, 667-686.

[00VIT] Vitorge P., Masella M. (2000) Chem. Phys. Letters, 333, 367-374.

[01LEM] Lemire R., Fuger J., Nitsche H., Rand M., Spahiu K., Sullivan J., Ullman W., Vitorge P. (2001) Chemical Thermodynamics of Neptunium and Plutonium. Paris OCDE AEN, Elsevier

[02DER] Derepas A.-L., Soudan J.-M., Brenner V., Dognon J.-P., Millié Ph. (2002) J.Comput. Chem., 23, 10, p.1013-1030

[02GOU] Gouze P., Coudrain-Ribstein A.(2002) Applied Geochemistry 17, 39-47

[02MIC] Michard G., (2002) Chimie des eaux naturelles : principes de géochimie des eaux. Paris Publisud 461 p ISBN 2-86600-890-1 (br.)

[02VIT] Vitorge P., Capdevila H., Maillard S., Fauré M.-H., Vercoüter T. (2002) J. Nuclear Sc. Techno. Supplement 3. p713-716. Oral presentation: Actinides 2001, International Conference Hayama, Japan November 4- 9, 2001

[03BEA] Beaucaire C., Pearson J. and Gautschi A. (2003) OECD workshop: geosphere stability, Braunschweig, Germany, 9-11 December 2003.



[03CLA] Clavaguéra-Sarrio C., Brenner V., Hoyau S., Marsden C. J., Millié P., Dognon J.-P. (2003) J. Phys. Chem. B, 107, p.3051-3060

[03GRE] Gresham G. L., Gianotto A. K., Harrington P. B., Cao L., Scott J. R., Olson J. E., Appelhans A. D., Van Stipdonk M. J. Groenewold, G. S. (2003) J. Phys. Chem. A, V 107, N 41 pp 8530 - 8538

[03VIT] Vitorge P., Capdevila H (2003). Radiochim. Acta 91, 623–631. CEA INSTN-Saclay. Invited conference: Journée d'information CETAMA, SEMINAIRE SPECIATION. 11/12/2001

[04DES] Descostes M., Vitorge P., Beaucaire C. (2004) Pyrite dissolution in acidic media. Geochim. Cosmochim. Acta (to be published).

[04PEL] Pellenq R. (2004) L'actualité chim. 273, 12-22 (in French)